Clinical Cancer Research

Dynamic Contrast-Enhanced Magnetic Resonance Imaging for Assessment of Antiangiogenic Treatment Effects in Multiple Myeloma

Maximilian Merz[1,2], Judith Ritsch[2], Christina Kunz[3], Barbara Wagner[2], Sandra Sauer[1], Dirk Hose[1], Thomas Moehler[1], Stefan Delorme[2], Hartmut Goldschmidt[1,4], Christian Zechmann[5], and Jens Hillengass[1,2]

Abstract

Purpose: To noninvasively assess bone marrow microcirculation before and after therapy in patients with newly diagnosed multiple myeloma with dynamic contrast-enhanced MRI (DCE-MRI).

Experimental Design: Ninety-six patients received DCE-MRI before and after primary treatment for newly diagnosed multiple myeloma. For the 91 evaluable patients, treatment consisted of high-dose therapy (HDT) with autologous stem cell transplantation (ASCT) in 82 patients and chemotherapy without ASCT in 9 patients. In addition, 33 healthy volunteers were imaged as the control group. Analysis of DCE-MRI was performed according to the two-compartment model by Brix to quantify amplitude A (associated with blood volume) and exchange rate constant k_{ep} (reflecting vessel permeability and perfusion).

Results: Nonresponders showed significantly higher A-values before the start of therapy compared with responders ($P = 0.02$). In both responders and nonresponders to therapy, A-values dropped significantly ($P = 0.004$ and <0.001, respectively) after primary therapy, whereas lower values for k_{ep} were found only in responders ($P < 0.001$). Depth of remission was significantly correlated to decreased bone marrow microcirculation: Patients in near complete response (nCR) or complete remission (CR) after treatment showed significantly lower values for A compared with patients not achieving nCR+CR. The application of HDT or novel agents had no significant effect on DCE-MRI parameters after therapy, although patients treated with novel agents more often achieved nCR+CR (42%/12.5%; $P < 0.002$). Higher k_{ep} -values at second MRI were positively correlated to shorter overall survival (HR 3.53; 95% confidence intervals, 1.21–10.33; $P = 0.02$).

Conclusion: Parameters from DCE-MRI are correlated to remission after primary therapy and outcome in newly diagnosed multiple myeloma. *Clin Cancer Res; 21(1); 106–12. ©2014 AACR.*

Introduction

In multiple myeloma, the interaction between malignant plasma cells and nonmalignant stromal cells causes several changes in the bone marrow microenvironment that are pivotal for the pathogenesis of the disease. The induction of angiogenesis by malignant plasma cells plays a major role in the transformation from nonmalignant precursor states like monoclonal gammopathy of undetermined significance (MGUS) and smoldering multiple myeloma (SMM) to symptomatic multiple myeloma (1, 2). Correspondingly, patients with multiple myeloma show a higher bone marrow microvessel density (MVD) than patients with SMM, MGUS, or healthy individuals (3). Increased bone marrow microcirculation is associated with adverse outcome in patients with multiple myeloma (4, 5) as well as SMM (6), and angiogenesis is directly linked to the development of multiple myeloma-related bone disease (7, 8). Furthermore, patients in remission after therapy showed a significantly decreased MVD compared with those with residual disease (9–11). In most of these studies, histologic evaluation of bone marrow biopsies was performed to quantify angiogenesis. However, bone marrow biopsies are obtained from a small anatomical region and will not be repeated unless clinically indicated. Therefore, there are only limited data available on how bone marrow microcirculation changes over time in patients with multiple myeloma receiving systemic therapy.

Imaging treatment response in multiple myeloma is an important but challenging task because lytic bone lesions only undergo subtle morphologic changes after treatment (12). Dynamic contrast-enhanced MRI (DCE-MRI) is a noninvasive imaging modality to study bone marrow microcirculation in patients with monoclonal plasma cell diseases (6, 13–15). In patients with solid tumors, it has become a valuable tool to quantify treatment response beyond measuring tumor size. However, there are only few studies including small numbers of heterogeneous patient groups that used DCE-MRI for the longitudinal assessment of antiangiogenic treatment response in multiple myeloma (16, 17).

[1]Department of Hematology and Oncology, University Hospital of Heidelberg, Heidelberg, Germany. [2]Department of Radiology, German Cancer Research Center, Heidelberg, Germany. [3]Division of Biostatistics, German Cancer Research Center, Heidelberg, Germany. [4]National Center for Tumor Diseases, Heidelberg, Germany. [5]Rinecker Proton Therapy Center, Munich, Germany.

Corresponding Author: Maximilian Merz, Department of Medicine V, University Hospital of Heidelberg, Im Neuenheimer Feld 410, 69120 Heidelberg, Germany. Phone: 49-6221-56-4781; Fax: 49-6221-56-4171; E-mail: maximilian.merz@med.uni-heidelberg.de

doi: 10.1158/1078-0432.CCR-14-1029

Translational Relevance

Angiogenesis has been identified as a pathogenic and prognostic factor in multiple myeloma. Dynamic contrast-enhanced MRI (DCE-MRI) is a noninvasive imaging method quantifying bone marrow microcirculation in patients with plasma cell diseases. Our study demonstrates that DCE-MRI enables the assessment of antiangiogenic treatment effects to primary therapy in patients with multiple myeloma. We showed that patients in remission exhibit significantly decreased A- and k_{ep}-values, which are surrogate markers for decreased bone marrow microcirculation. Furthermore, nonresponders exhibited higher baseline A-values than responders, and higher k_{ep}-values after therapy are associated with shorter overall survival. Imaging treatment response in multiple myeloma nowadays is mainly based on the assessment of morphologic changes upon therapy. Because morphologic changes, especially of osteolysis, rarely occur shortly after therapy, DCE-MRI is useful for imaging early treatment response in multiple myeloma.

We therefore performed this prospective trial applying DCE-MRI in patients before and after therapy under the hypothesis that changes in bone marrow microcirculation are correlated to remission and outcome in newly diagnosed multiple myeloma. Furthermore, we investigated whether baseline parameters from DCE-MRI might predict treatment response.

Patients and Methods

Patients

After written informed consent, 96 patients with newly diagnosed multiple myeloma were recruited between November 2004 and April 2011 to receive DCE-MRI before the start of systemic treatment and after the first-line of therapy. The study was approved by the institutional ethics committee. No prior systemic therapy for multiple myeloma was allowed before the first DCE-MRI. Five patients had to be excluded from the analysis as they had been assigned to second-line treatment before second MRI because of progression during first-line therapy. Patient characteristics at first DCE-MRI are summarized in Table 1. Median time from first to second MRI was 14 months. There were three patients with >30 months from first to second MRI. They were included in the analysis because they remained in remission and did not receive further therapy beyond first-line treatment. In addition, 33 healthy individuals (16 female, 17 male, median age 56 years) were included in our study as control group after written informed consent was obtained.

Imaging protocol and analysis

MRI was performed on a 1.5 Tesla MRI (Magnetom Symphony, Siemens Medical Solution) equipped with a spine coil for radiofrequency excitation and detection as described previously (6). For DCE-MRI, we used a saturation recovery TurboFLASH-Sequence in sagittal orientation covering the lumbar spine (TR/TE 79/4.76 ms, FOV 380 mm, 9 slices, 8 mm slice thickness, voxel size $1.5 \times 1.5 \times 8$ mm, flip angle 80°, total acquisition time: 5 minutes 54 seconds). After the first four measurements, 0.1 mmol/kg Gadolinium-DTPA (Magnevist, Bayer Schering Pharma) was intravenously infused via a cannula placed in an antecubital vein with an automated injection system (Spectris Solaris, Medrad). Image postprocessing and analysis were performed according to the two-compartment model proposed by Brix and colleagues with the MeVislab software (MeVis Medical Solutions AG) to calculate amplitude A (arbitrary units) and exchange rate constant k_{ep} (min^{-1}; ref. 18). In the Brix model, amplitude A is mainly influenced by the distribution space of the contrast agent and therefore a surrogate for blood volume, while k_{ep} reflects both, vessel permeability and perfusion (19). Pixel-based analysis of both parameters was performed in manually selected regions of interest (ROI). Investigators were blinded to patients' remission and outcome. To minimize interobserver variability, the selected ROIs contained the whole bone marrow of lumbar vertebral bodies that was identified on unenhanced T1-weighted images. In that way, values of 455 vertebral bodies were assessed before and after therapy. Because degenerative changes like osteochondrosis, Schmorl's nodes, or anatomical variants like a prominent basivertebral vein can cause changes that might mimic plasma cell infiltration, these structures were not included in the respective ROIs. Overall, 21 vertebral bodies had to be excluded from the analysis because of these changes. The Brix model was applied because it had been shown to be more robust than the also established model proposed by Tofts and colleagues (19).

Treatment

High-dose therapy (HDT) followed by autologous stem cell transplantation (ASCT) was performed in 82 patients. Single HDT was performed in 39 cases, whereas 43 patients received tandem

Table 1. Patient characteristics, overview of treatment, and response to primary therapy

Characteristic	Median	Range
Age	58	35–80
Hemoglobin	11.9	7.4–16.4
Calcium	2.3	1.9–4.4
Creatinine	0.9	0.5–2.5
β-2 microglobulin	2.6	1.1–16.9
Albumin	39.7	29.3–53.5
LDH	186	102–341
M-protein	36.2	0–89.0
Characteristic		***n* (%)**
Sex (female)		33 (36)
Type of M-protein		
IgG		63 (69)
IgA		16 (18)
Bence Jones		9 (10)
Other		5 (5)
CRAB criteria		
Hypercalcemia		4 (4)
Renal insufficiency		1 (1)
Anemia		14 (15)
Bone disease		68 (75)
Therapy		
HDT		
None		9 (10)
Single		39 (43)
Tandem		43 (47)
Novel agents		
Yes		50 (55)
No		41 (45)
Remission after primary therapy (2nd DCE-MRI)		
nCR+CR		26 (29)
VGPR+PR+MR		55 (61)
SD-PD		9 (10)

HDT. Patients treated with HDT received a median of three-cycle (range 2–4) induction chemotherapy consisting of either vincristin (VAD, $n = 34$ patients), bortezomib (PAD, $n = 34$), or thalidomide (TAD, $n = 10$) in combination with adriamycine and dexamethasone. In one patient receiving bortezomib as induction therapy, adriamycine was replaced by cyclophosphamide, 2 patients received only adriamycine/dexamethasone, and one patient was treated with ifosfamide/dexamethasone before HDT. In patients, who were candidates for HDT, induction therapy was followed by a cycle of cyclophosphamide, adriamycine, and dexamethasone (CAD) as mobilization chemotherapy and G-CSF application for peripheral stem cell harvest. In one patient, ifosfamide was used as mobilization chemotherapy and in another patient, an antagonist against CXCR4 was used for stem cell mobilization. Out of 9 patients who were not eligible for HDT, 8 were treated with melphalan/prednisone (MP) alone ($n = 3$), in combination with bortezomib ($n = 4$) or thalidomide ($n = 1$). One patient, not eligible for HDT, received three-cycle VAD followed by two-cycle bortezomib/dexamethasone. Table 1 gives a summary of the applied chemotherapy.

Follow-up

All patients were seen in our outpatient clinic every 3 to 6 months after the initial diagnosis, including physical examinations, routine blood work, serum electrophoresis, and urine analysis. For HDT with ASCT, patients were admitted to our ward. After discharge, patients presented again in our outpatient clinic for assessment of treatment response according to the guidelines of the International Myeloma Working Group (IMWG) and for the second DCE-MRI. IMWG response criteria were modified to include near complete response (nCR). Patients were stratified into three groups according to how they had responded to therapy: Group 1 = near complete response and complete remission (nCR+CR); Group 2 = very good partial remission, partial remission, or minimal response (VGPR+PR+MR); Group 3 = stable disease or progressive disease (SD+PD). Patients in group 1 and 2 were considered responders to therapy; patients in group 3 were classified as nonresponders.

Statistical analysis

Fisher exact test was used to compare remission rates according to applied therapies. A- and k_{ep}-values of ROIs from the five vertebral bodies of the lumbar spine were summarized for each patient as median values. Median k_{ep}-values were log-transformed before the analysis. Because previous studies showed that k_{ep} values can only be determined reliably for values ≤ 13 minutes^{-1}, values >13 minutes^{-1} were truncated at 13 minutes^{-1}. To assess changes in DCE-MRI parameters A and k_{ep} before and after therapy for responders and nonresponders, the paired Wilcoxon signed-rank test was performed. The distribution of median A- and k_{ep}-values was compared between the different remission categories using Wilcoxon rank-sum tests. Differences and trends for A and k_{ep} in the remission categories after therapy were analyzed using the Kruskal–Wallis test and the Jonckheere–Terpstra trend test. Multivariate linear models accounting for baseline DCE-MRI values at first MRI, the application of novel agents, and HDT were used to analyze the impact of these factors on the change of A/k_{ep} between the first and second DCE-MRI. Furthermore, multivariate logistic regression models were applied for modeling dichotomized response to therapy in dependency of baseline A/k_{ep}-values at first MRI, changes in A/k_{ep}-values between first and second MRI as well as the application of novel agents and HDT. Cox models were fitted to investigate the prognostic value of median A/k_{ep} at the second MRI for progression-free (PFS) and overall survival (OS). PFS and OS were calculated starting from time of the second MRI. P values <0.05 were considered statistically significant. Data analysis was performed using SPSS 20 (IBM) and R versions 2.15.3 and 3.1.1 (http://cran.r-project.org/).

Results

Response to treatment

Out of the 91 patients, 26 patients (29%) had achieved nCR+CR at the time point of the second MRI and 55 patients (61%) achieved MR, PR, or VGPR. Therefore, 81 patients (90%) were considered as responders to therapy, whereas 9 patients showed stable or progressive disease at the second DCE-MRI and were classified as nonresponders. In one patient with nonsecretory multiple myeloma the remission after primary therapy could not be defined according to IMWG criteria. Rates of nCR+CR were not significantly different between patients eligible (28.4%) or not eligible for HDT (33.3%, $P = 0.80$). Patients, either eligible or not eligible for HDT, that were treated with thalidomide or bortezomib achieved significantly more often nCR+CR (42.0%) compared with patients treated with neither of these agents (12.5%, $P = 0.002$). Remission after primary therapy is summarized in Table 1.

DCE-MRI parameters before and after treatment in responders and nonresponders to therapy

Nonresponders showed significantly higher median values for amplitude A before the start of treatment compared with responders to therapy ($P = 0.02$; Fig. 1A). No significant differences between the two groups were found for median exchange rate constant k_{ep} before therapy ($P = 0.52$; Fig. 1B). In nonresponders to therapy, the second DCE-MRI revealed a significantly lower median amplitude A compared with initial values ($P = 0.004$; Fig. 1A), while no significant changes were found for median k_{ep}-values ($P = 0.20$; Fig. 1B). The observed effects on A and k_{ep} were more pronounced in patients responding to therapy: Responders showed significantly lower median values for A ($P < 0.001$; Fig. 1A) and k_{ep} ($P < 0.001$; Fig. 1B). Figure 1 depicts all measured DCE-MRI values. Figure 2 gives an example of representative color maps for A and k_{ep} before and after successful therapy.

DCE-MRI parameters after treatment according to remission after therapy

The comparison of DCE-MRI parameters from patients in nCR+CR after therapy with patients achieving VGPR+PR+MR or with patients not responding to therapy revealed the following differences among the groups (Fig. 3): Patients in nCR+CR showed significantly lower median A-values after treatment compared with patients with VGPR+PR+MR ($P = 0.012$) and SD+PD ($P = 0.03$) since median values dropped to same levels as in healthy individuals (Fig. 3A, respectively). In addition, patients with SD+PD had higher median A-values after therapy than patients in VGPR+PR+MR ($P < 0.001$; Fig. 3A). No significant differences were found for median exchange rate constant k_{ep} among the three different groups (Fig. 3B). Jonckheere–Terpstra trend tests, which examine the association of ordered categorical response with the median DCE-MRI values at second MRI, showed a significant

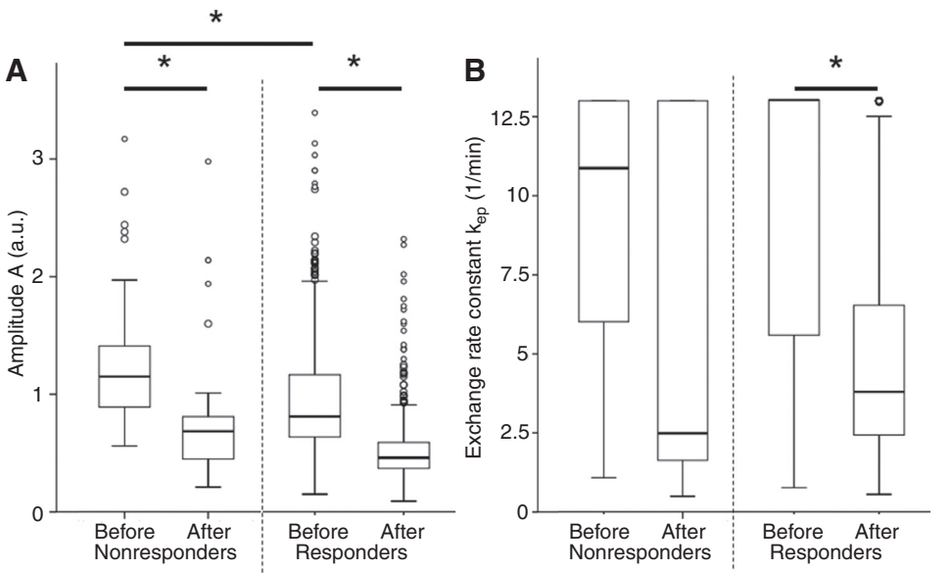

Figure 1.
Boxplots of DCE-MRI parameters A (A) and k_{ep} (B) before and after primary therapy for responders and nonresponders. The box depicts the interquartile range, with the median value as a line. Whiskers show 10th and 90th percentiles, and outliers are depicted separately. The symbol "*" denotes significant differences between the groups.

association with median A-values at second MRI ($P = 0.003$). When testing the association between values measured at the second DCE-MRI and the application of HDT or thalidomide and bortezomib, no significant results were obtained.

Multivariate analysis of DCE-MRI parameters and response

Multivariate linear models demonstrated that neither the application of novel agents nor HDT had a significant impact on changes in median A/k_{ep}-values between the first or second MRI. Higher median A/k_{ep}-values at first MRI were significantly associated with smaller changes between the first and second DCE-MRI ($P < 0.001$, respectively).

In the multivariate logistic regression model of dichotomized response including median A-values at first MRI and change in median A-values, the application of tandem HDT was the only significant prognostic factor [$P = 0.01$; OR: 14.1; 95% confidence intervals (CI), 1.5–130.2)]. However, a negative trend of higher median A-values at first MRI on response to therapy was observed ($P = 0.08$; OR: 0.4; 95% CI, 0.1–3.2).

In the multivariate logistic regression model including log-transformed median k_{ep}-values at first MRI and change in log-transformed median k_{ep}-values, the only prognostic factor was application of tandem HDT as well ($P = 0.006$; OR: 15.6; 95% CI, 1.9–128.8).

Survival analysis

Median follow-up was 39.0 months with a median PFS of 20.1 months after second MRI. Median OS was not reached. Survival analysis revealed that higher median k_{ep}-values at the second MRI resulted in shorter OS (HR 3.53; 95% CI, 1.21–10.33; $P = 0.02$). These changes were also associated with shorter PFS but did not reach statistical significance (HR 1.37; 95% CI, 0.85–2.18; $P = 0.19$). No significant results were obtained for amplitude A.

Discussion

In our current prospective study, we performed DCE-MRI before and after primary therapy in patients with newly diagnosed multiple myeloma to longitudinally assess changes in bone marrow microcirculation and correlate findings with treatment response. We demonstrate for the first time that responders exhibit significantly lower values for amplitude A and exchange rate constant k_{ep} compared with nonresponders after therapy and higher k_{ep}-values after therapy are associated with shorter OS. Furthermore, depth of remission was significantly correlated to lower A-values and patients not responding to therapy showed higher A-values before the start of therapy compared with responders. Previous studies indicated that the induction of angiogenesis is crucial for the progression from MGUS and SMM to symptomatic multiple myeloma (1, 3) and response to treatment is accompanied by decreased MVD (9–11). We noninvasively confirmed these findings and showed that a reduction of tumor burden is not only accompanied by drop of blood volume (lower A-values), but also reduced vessel permeability (lower k_{ep}-values). This is in line with preclinical and clinical studies in solid tumors demonstrating that antiangiogenic treatment effects are not only limited to vessel regression, but also functional normalization of tumor vasculature (20).

Since the introduction of thalidomide, bortezomib, and lenalidomide, it has been argued whether the improved outcome compared with conventional chemotherapy might be due to the antiangiogenic properties of the respective agents (21). In the case of immunomodulatory drugs, antiangiogenesis has been described as one of the versatile effects on the bone marrow microenvironment (22). Bortezomib exhibited antiangiogenic properties in preclinical studies as well (23). A remaining question is, whether vessel regression upon therapy is due to antiangiogenic therapy effects or just an epiphenomenon of successful myeloma treatment. In our current study, treatment with novel agents or tandem HDT improved remission compared with conventional chemotherapy but was not associated with lower DCE-MRI parameters in multivariate analysis. Because depth of remission was associated with lower A-values after primary therapy, we suppose that the observed normalization of microcirculation in patients achieving nCR+CR might have been rather a consequence than a prerequisite for successful treatment. In line with these results, we

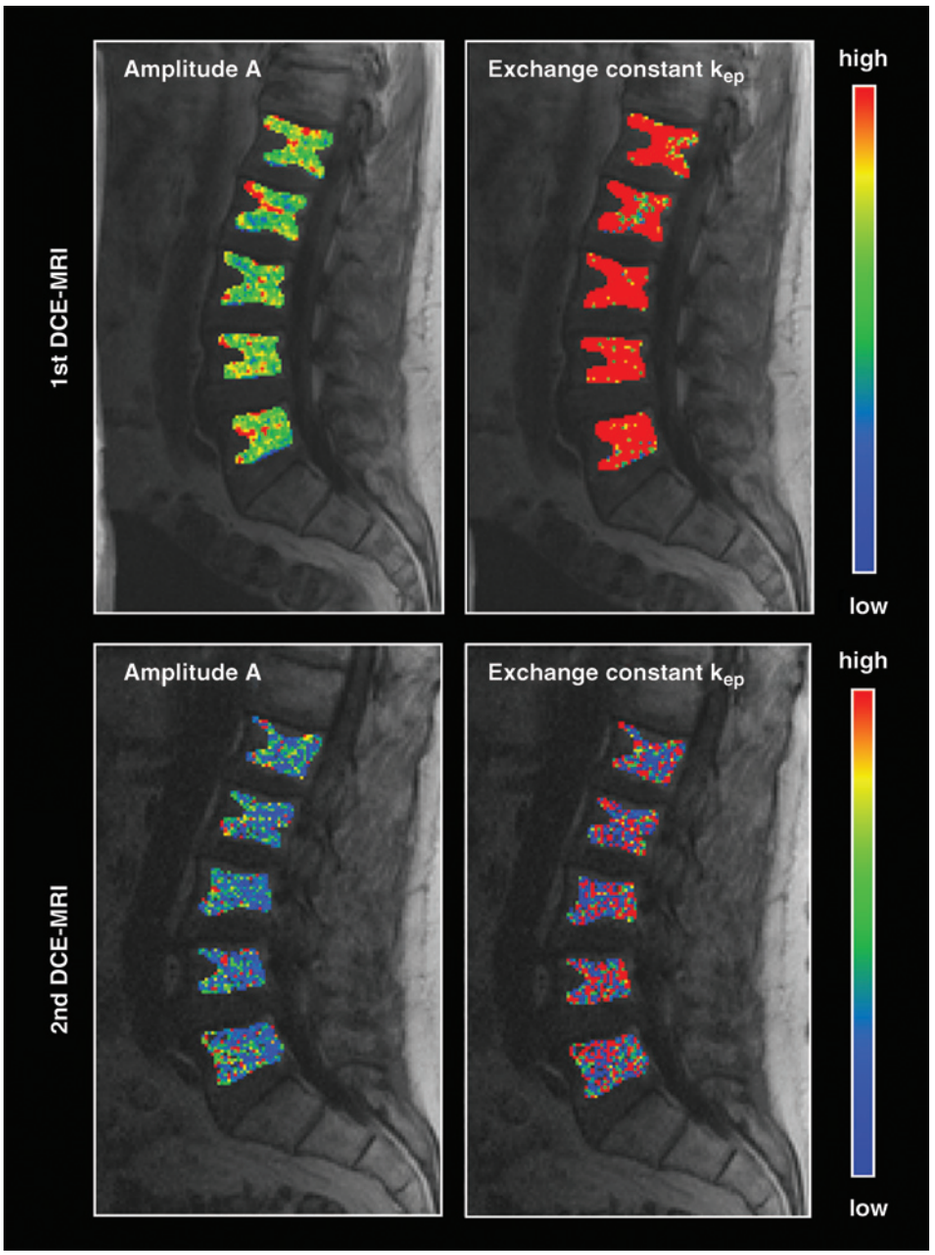

Figure 2.
Representative color maps for parameters A and k_{ep} before and after successful primary therapy. Values range from high (red) to low (blue).

found also in nonresponders, lower A-values after therapy compared with the initial measurements, which might indicate that vessel regression alone does not automatically translate into reduction of tumor burden. Although this assumption needs to be clarified by further studies, recent clinical trials with antiangiogenic monoclonal antibodies or tyrosine kinase inhibitors as single agents or in combination with bortezomib as well as lenalidomide failed to show additional benefit in patients with relapsed or refractory multiple myeloma (24–27).

Beyond the observed correlation between bone marrow microcirculation and remission after therapy, we found that nonresponders had significantly higher baseline A-values than responders. In addition, in patients with higher baseline A/k_{ep}-values, the treatment-induced drop was less pronounced than in patients with lower baseline values. Therefore, DCE-MRI before the start of therapy might have predictive and prognostic implications. This assumption is supported by a recent study, which demonstrated that proangiogenic factors lead to drug resistance and relapse in patients with multiple myeloma (28).

Imaging treatment response in multiple myeloma is challenging because morphologic changes of existing bone lesions seldom occur after therapy (29). With our study, we were able to assess treatment response based on quantitative parameters, which is less influenced by interobserver variability than

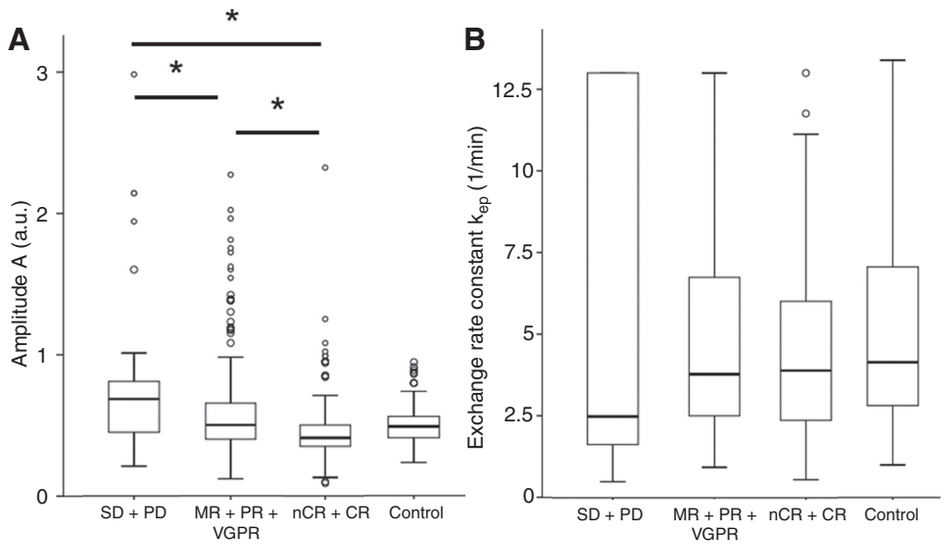

Figure 3.
Boxplots of DCE-MRI parameters A (A) and k_{ep} (B) according to remission after primary therapy and for healthy individuals (controls). The box depicts the interquartile range, with the median value as a line. Whiskers show 10th and 90th percentiles, and outliers are depicted separately. The symbol "*" denotes significant differences between the groups.

morphologic evaluation of osteolyses. This is of particular interest for the assessment of treatment response in nonsecretory myeloma or patients with extramedullary disease. In addition, DCE-MRI might also help to detect viable tumor tissue within preexisting osteolyses and to identify candidates for local therapy. This theory is supported by findings from a small study that linked high values for amplitude A to increased fracture risk during follow-up (30). Furthermore, DCE-MRI offers the opportunity to image treatment response in asymptomatic patients without osteolyses which might become attractive in the future with the emerging role of treating patients with high-risk SMM (31).

There are major downsides to the current study that need to be addressed in future trials of DCE-MRI in multiple myeloma. To investigate early treatment effects, follow-up examinations with DCE-MRI need to be scheduled at earlier time points and not only at the end of primary therapy as in the current study. This might clarify if changes in bone marrow microcirculation precede or just parallel the reduction of tumor burden. Since recruitment for this trial started in 2004 and ended in 2011, patients enrolled at later time points were more likely to be treated with novel agents during induction therapy. This might have influenced the prognostic evaluation of DCE-MRI on PFS and to a lesser degree on OS, because novel agents were already available for treatment of relapsed disease in 2004. In addition, the prognostic value of DCE-MRI in multiple myeloma needs to be confirmed in a larger cohort of patients, not only with symptomatic disease, but also MGUS and SMM.

In summary, we demonstrate that longitudinal assessment of bone marrow microcirculation with DCE-MRI correlates with treatment response in multiple myeloma and has prognostic implications in newly diagnosed patients.

Disclosure of Potential Conflicts of Interest

No potential conflicts of interest were disclosed.

Authors' Contributions

Conception and design: J. Ritsch, T. Moehler, S. Delorme, C. Zechmann, J. Hillengass
Development of methodology: J. Ritsch, S. Delorme
Acquisition of data (provided animals, acquired and managed patients, provided facilities, etc.): J. Ritsch, B. Wagner, S. Sauer, D. Hose, H. Goldschmidt, J. Hillengass
Analysis and interpretation of data (e.g., statistical analysis, biostatistics, computational analysis): M. Merz, J. Ritsch, C. Kunz, D. Hose, T. Moehler, S. Delorme, C. Zechmann, J. Hillengass
Writing, review, and/or revision of the manuscript: M. Merz, J. Ritsch, C. Kunz, D. Hose, T. Moehler, S. Delorme, H. Goldschmidt, C. Zechmann, J. Hillengass
Administrative, technical, or material support (i.e., reporting or organizing data, constructing databases): B. Wagner
Study supervision: M. Merz, B. Wagner, T. Moehler, S. Delorme, J. Hillengass

Grant Support

This work was supported by grants from the Dietmar-Hopp-Stiftung, the Deutsche José Carreras Leukämie-Stiftung e.V., and the Deutsche Forschungsgemeinschaft (SFB Transregio 79).

The costs of publication of this article were defrayed in part by the payment of page charges. This article must therefore be hereby marked *advertisement* in accordance with 18 U.S.C. Section 1734 solely to indicate this fact.

Received April 24, 2014; revised September 11, 2014; accepted October 8, 2014; published OnlineFirst October 28, 2014.

References

1. Hose D, Moreaux J, Meissner T, Seckinger A, Goldschmidt H, Benner A, et al. Induction of angiogenesis by normal and malignant plasma cells. Blood 2009;114: 128–43.
2. Kumar S, Witzig TE, Timm M, Haug J, Wellik L, Kimlinger TK, et al. Bone marrow angiogenic ability and expression of angiogenic cytokines in myeloma: evidence favoring loss of marrow angiogenesis inhibitory activity with disease progression. Blood 2004;104: 1159–65.
3. Rajkumar SV, Mesa RA, Fonseca R, Schroeder G, Plevak MF, Dispenzieri A, et al. Bone marrow angiogenesis in 400 patients with monoclonal

gammopathy of undetermined significance, multiple myeloma, and primary amyloidosis. Clin Cancer Res 2002;8: 2210–6.
4. Kumar S, Gertz MA, Dispenzieri A, Lacy MQ, Wellik LA, Fonseca R, et al. Prognostic value of bone marrow angiogenesis in patients with multiple myeloma undergoing high-dose therapy. Bone Marrow Transplant. 2004;34: 235–9.
5. Rajkumar SV, Leong T, Roche PC, Fonseca R, Dispenzieri A, Lacy MQ, et al. Prognostic value of bone marrow angiogenesis in multiple myeloma. Clin Cancer Res 2000;6: 3111–6.
6. Hillengass J, Zechmann C, Bauerle T, Wagner-Gund B, Heiss C, Benner A, et al. Dynamic contrast-enhanced magnetic resonance imaging identifies a subgroup of patients with asymptomatic monoclonal plasma cell disease and pathologic microcirculation. Clin Cancer Res 2009;15: 3118–25.
7. Tanaka Y, Abe M, Hiasa M, Oda A, Amou H, Nakano A, et al. Myeloma cell-osteoclast interaction enhances angiogenesis together with bone resorption: a role for vascular endothelial cell growth factor and osteopontin. Clin Cancer Res 2007;13: 816–23.
8. Storti P, Bolzoni M, Donofrio G, Airoldi I, Guasco D, Toscani D, et al. Hypoxia-inducible factor (HIF)-1alpha suppression in myeloma cells blocks tumoral growth *in vivo* inhibiting angiogenesis and bone destruction. Leukemia 2013;27: 1697–706.
9. Kumar S, Witzig TE, Dispenzieri A, Lacy MQ, Wellik LE, Fonseca R, et al. Effect of thalidomide therapy on bone marrow angiogenesis in multiple myeloma. Leukemia 2004;18: 624–7.
10. Rana C, Sharma S, Agrawal V, Singh U. Bone marrow angiogenesis in multiple myeloma and its correlation with clinicopathological factors. Ann Hematol 2010;89: 789–94.
11. Sezer O, Niemoller K, Kaufmann O, Eucker J, Jakob C, Zavrski I, et al. Decrease of bone marrow angiogenesis in myeloma patients achieving a remission after chemotherapy. Eur J Haematol 2001;66: 238–44.
12. Tan E, Weiss BM, Mena E, Korde N, Choyke PL, Landgren O. Current and future imaging modalities for multiple myeloma and its precursor states. Leuk Lymphoma 2011;52: 1630–40.
13. Nosas-Garcia S, Moehler T, Wasser K, Kiessling F, Bartl R, Zuna I, et al. Dynamic contrast-enhanced MRI for assessing the disease activity of multiple myeloma: a comparative study with histology and clinical markers. J Magn Reson Imaging 2005;22: 154–62.
14. Hillengass J, Wasser K, Delorme S, Kiessling F, Zechmann C, Benner A, et al. Lumbar bone marrow microcirculation measurements from dynamic contrast-enhanced magnetic resonance imaging is a predictor of event-free survival in progressive multiple myeloma. Clin Cancer Res 2007;13: 475–81.
15. Bhutani M, Turkbey B, Tan E, Kemp TJ, Pinto LA, Berg AR, et al. Bone marrow angiogenesis in myeloma and its precursor disease: a prospective clinical trial. Leukemia 2014;28: 413–6.
16. Lin C, Luciani A, Belhadj K, Deux JF, Kuhnowski F, Maatouk M, et al. Multiple myeloma treatment response assessment with whole-body dynamic contrast-enhanced MR imaging. Radiology 2010;254: 521–31.
17. Dutoit JC, Vanderkerken MA, Verstraete KL. Value of whole body MRI and dynamic contrast enhanced MRI in the diagnosis, follow-up and evaluation of disease activity and extent in multiple myeloma. Eur J Radiol 2013;82: 1444–52.
18. Brix G, Semmler W, Port R, Schad LR, Layer G, Lorenz WJ. Pharmacokinetic parameters in CNS Gd-DTPA enhanced MR imaging. J Comput Assist Tomogr 1991;15: 621–8.
19. Zwick S, Brix G, Tofts PS, Strecker R, Kopp-Schneider A, Laue H, et al. Simulation-based comparison of two approaches frequently used for dynamic contrast-enhanced MRI. Eur Radiol 2010;20: 432–42.
20. Jain RK. Normalizing tumor microenvironment to treat cancer: bench to bedside to biomarkers. J Clin Oncol 2013;31: 2205–18.
21. Anargyrou K, Dimopoulos MA, Sezer O, Terpos E. Novel anti-myeloma agents and angiogenesis. Leuk Lymphoma 2008;49: 677–89.
22. Otjacques E, Binsfeld M, Noel A, Beguin Y, Cataldo D, Caers J. Biological aspects of angiogenesis in multiple myeloma. Int J Hematol 2011;94: 505–18.
23. Roccaro AM, Hideshima T, Raje N, Kumar S, Ishitsuka K, Yasui H, et al. Bortezomib mediates antiangiogenesis in multiple myeloma via direct and indirect effects on endothelial cells. Cancer Res 2006;66: 184–91.
24. Somlo G, Lashkari A, Bellamy W, Zimmerman TM, Tuscano JM, O'Donnell MR, et al. Phase II randomized trial of bevacizumab versus bevacizumab and thalidomide for relapsed/refractory multiple myeloma: a California Cancer Consortium trial. Br J Haematol 2011;154: 533–5.
25. Prince HM, Honemann D, Spencer A, Rizzieri DA, Stadtmauer EA, Roberts AW, et al. Vascular endothelial growth factor inhibition is not an effective therapeutic strategy for relapsed or refractory multiple myeloma: a phase 2 study of pazopanib (GW786034). Blood 2009;113: 4819–20.
26. Kovacs MJ, Reece DE, Marcellus D, Meyer RM, Mathews S, Dong RP, et al. A phase II study of ZD6474 (Zactima, a selective inhibitor of VEGFR and EGFR tyrosine kinase in patients with relapsed multiple myeloma–NCIC CTG IND.145. Invest New Drugs 2006;24: 529–35.
27. White D, Kassim A, Bhaskar B, Yi J, Wamstad K, Paton VE. Results from AMBER, a randomized phase 2 study of bevacizumab and bortezomib versus bortezomib in relapsed or refractory multiple myeloma. Cancer 2013;119: 339–47.
28. Ria R, Catacchio I, Berardi S, De Luisi A, Caivano A, Piccoli C, et al. HIF-1alpha of bone marrow endothelial cells implies relapse and drug resistance in patients with multiple myeloma and may act as a therapeutic target. Clin Cancer Res 2014;20: 847–58.
29. Mena E, Choyke P, Tan E, Landgren O, Kurdziel K. Molecular imaging in myeloma precursor disease. Semin Hematol 2011;48: 22–31.
30. Scherer A, Wittsack HJ, Strupp C, Gattermann N, Haas R, Modder U. Vertebral fractures in multiple myeloma: first results of assessment of fracture risk using dynamic contrast-enhanced magnetic resonance imaging. Ann Hematol 2002;81: 517–21.
31. Mateos MV, Hernandez MT, Giraldo P, de la Rubia J, de Arriba F, Lopez Corral L, et al. Lenalidomide plus dexamethasone for high-risk smoldering multiple myeloma. N Engl J Med 2013;369: 438–47.